Available online at www.sciencedirect.com
SCIENCE DIRECT®
Solar Energy Materials & Solar Cells
ELSEVIER
Solar Energy Materials & Solar Cells 77 (2003) 319–330
www.elsevier.com/locate/solmat

Letters

Structure and photoelectrochemical properties of ruthenium(II) polypyridyl complexes as sensitizers for nanocrystalline TiO_2 electrodes

Qiao-Hong Yao[a], Yan-Yi Huang[a], Lin-Qing Song[b], Bao-Wen Zhang[b], Chun-Hui Huang[a,*], Zhong-Sheng Wang[a], Fu-You Li[a], Xin-Sheng Zhao[c]

[a] *State Key Laboratory of Rare Earth Materials Chemistry and Applications, Peking University, Beijing 100871, People's Republic of China*
[b] *Technology Institute of Physics and Chemistry, Chinese Academy of Science, Beijing 100101, People's Republic of China*
[c] *Institute of Physical Chemistry, Peking University, Beijing 100871, People's Republic of China*

Abstract

The relationship between the structures and photoelectrochemical properties of two dyes, cis-dithiocyanato-N,N′-bis(4,4′-dicarboxyl-2,2′-bipyridyl) Ru(II) and cis-dithiocyanato-(4,4′-dicarboxyl-2,2′-bipyridyl)-(4,4′-di((N,N′-methylphenylamino)methylene)-2,2′-bipyridyl) Ru(II), was examined and compared under the same conditions. Data show that the photophysical properties (including molar extinction coefficients ε and excited-state lifetimes) and photoelectrochemical properties (including short-circuit photocurrent, open-circuit photovoltage, incident monochromatic photon to current conversion efficiency, overall energy conversion yield (η) and transient photocurrent) were changed greatly only due to an acceptor replaced by a donor in one of polypyridyl of the Ru(II) complex, suggesting that the molecular design in energy conversion is very sensitive.

Keywords: Photoelectric conversion; Polypyridyl complex; Sensitization; Nanocrystalline TiO_2

1. Introduction

Dye-sensitized Photoelectrochemical cells or Grätzel-type cells present a promising strategy for solar energy conversion, with energy conversion efficiency as high as

*Corresponding author. Tel.: +86-10-62757156; fax: +86-10-62751708.
E-mail address: hch@chem.pku.edu.cn (C.-H. Huang).

0927-0248/03/$ - see front matter
doi:10.1016/S0927-0248(03)00016-3

10% reported using the transition-metal sensitizer cis-dithiocyanato-N,N′-bis(4,4′dicarboxyl-2,2′-bipyridyl) Ru(II) (N3) [1,2]. Even though this record efficiency has not been broken for several years, the challenge to further improve overall quality of this kind of solar cells still remains. So many researchers are studying extensively on modifications of the three main components of the cell, i.e., the mesoporous oxide semiconductor [3–5], the photosensitizer [6–11], and the electrolyte [12–17]

The spectral and redox properties of ruthenium polypyridyl complexes qcan be tuned in two ways [6]. First, by introducing a ligand with a low-lying π^* molecular orbital and second by destabilization of the metal t_{2g} orbital through the introduction of a strong donor ligand. It is well known that N3 anchored to the TiO_2 surface by one carboxylated bippyridyl ligand. So it is reasonable to do some modification on the other carboxylated bippyridyl ligand and not affect the dye's adsorbing property. Bearing this idea, we synthesized cis-dithiocyanato-(4,4′-dicarboxyl-2,2′-bipyridyl)-(4,4′-di((N,N′-methylphenylamino)methylidene)-2,2′-bipyridyl) Ru(II) (mN3) by introducing the electron donor group $–CH_2N(CH_3)(C_6H_5)$, into the standard dye N3 to replace the electron acceptor group, –COOH, and compared its photoelectrical properties as sensitizer in Grätzel-type solar cells with that of N3. The molecular structures of N3 and mN3 are shown in Scheme 1.

2. Experimental details

2.1. Materials

Optically transparent conducting glass (CTO glass, fluorine-doped SnO_2 overlayer, transmission $>70\%$ in the visible, sheet resistance $30\,\Omega\,sq^{-1}$) was obtained from the Institute of Nonferrous Metals of China. Titanium tetraisopropoxide and

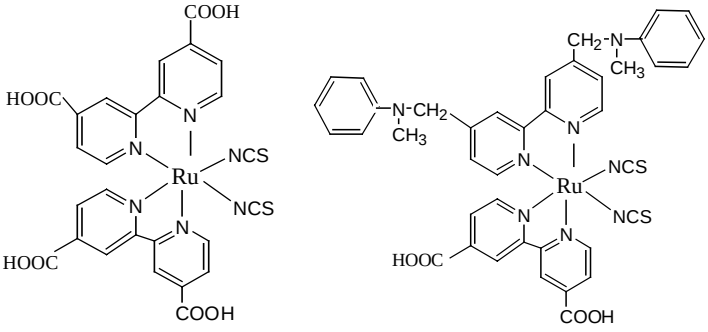

N3 **mN3**

Scheme 1. Molecular structures of N3 and mN3.

propylene carbonate (PC) were purchased from Acros. All other solvents and chemicals used in this work were reagent grade (Beijing chemical factory, China) and used without further purification. The redox electrolyte used is entirely 0.5 mol dm^{-3} LiI + 0.05 mol dm^{-3} I_2 in PC/acetonitrile (1:1 by volume).

The preparation of the dye mN3 will be reported elsewhere [18], and its purity is confirmed by ^{1}H NMR and elemental analysis.

2.2. Preparation of electrodes

Conducting glass substrates were pretreated prior to the preparation of nanocrystalline TiO_2 electrode according to the Ref. [19]. The CTO glass substrates were immersed in a saturated solution of KOH in 2-propanol overnight, rinsed with acetone, ethanol and doubly deionized water successively, and dried in an air stream. The total amount of 100–150 mg dm^{-3} TiO_2 colloidal was prepared following the procedure reported in literature 2. In order to improve the ohmic contact between TiO_2 particles and CTO glass, three drops of 1.5×10^{-3} mol dm^{-3} titanium tetraisopropoxide in 2-propanol was spread onto the conducting glass (2 cm × 8 cm) cm) and dried naturally in air at room temperature. Nanostructured TiO_2 films were fabricated by spreading the adhesive TiO_2 colloid onto the CTO glass and annealed at 450°C for 30 min. Repeating this procedure until the thickness required is achieved. Film thickness was determined with DEKTAK 3 profilometer.

Coloration of the TiO_2 surface with the dyes was carried out by immersing the film (still hot, i.e., 80°C) for 12 h in a 3×10^{-4} mol dm^{-3} solution of the dye in ethanol. After completion of the dye adsorption, the electrode was withdrawn from the solution, washed with ethanol, and dried under a stream of hot air. The amount of adsorbed dye was determined by measuring the concentration change of the dye solution before and after adsorption.

2.3. Photoelectrochemical measurement

The photoelectrochemical experiments were performed in a standard 2-electrode-system described elsewhere [2]. The dye-coated film was used as working electrode with effective area of 0.14 cm^2. The counter electrode was ITO glass on which 200 nm thick layer of Pt was deposited by sputtering. A thin layer sandwich-type solar cell was fabricated by clamping both electrodes tightly and then by introducing one drop of the redox electrolyte into the interelectrode space. A 500 W xenon lamp (Ushio Electric, Japan) served as a light source. A set of band-pass filters (Schott,USA) was set into the path of the excitation beam to adjust the excitation wavelength. Light intensities were measured with a Light Gauge Radiometer/Photometer (Coherent, USA). A KG-4 filter was used to filter off infrared light protecting the electrode from heating, a GG420 cut-off filter was used to cut off the light with wavelength less than 420 nm avoiding the excitation of TiO_2 by ultraviolet light, and a sheet of CTO glass was used to deduct the absorption of the support glass.

2.4. Instrumentation

The UV–vis spectra were measured with a Shimadzu model 3100UV-VIS-NIR spectrophotometer. A GCR-4 Nd:YAG Laser (Spectra Physics,USA) was employed for emission lifetime and transient current measurement. The laser pulse width is 6 ns. Transient photocurrent generation was recorded on a TDS 3032 Oscilloscope (Tektronix,USA). Synchrotron radiation photoelectron spectroscopy (SRPES) was measured on a photon–electron spectrometer (vsw Scientific Instruments Ltd., Eng.) through synchrotron radiation. Under ultra-vaccum (3.5×10^{-8} Pa), photon–electron spectra were recorded under 18.7 eV synchrotron radiation light, from which the first ionization energy, i.e., the HOMO energy level of the dye, was derived.

3. Results and discussion

3.1. Adsorption behavior

A nanocrystalline TiO_2 film was soaked into the mN3 solution in ethanol, and withdrawn from the solution for absorbance determination at variable time intervals. The sensitized film was washed thoroughly with anhydrous ethanol and dried in an airflow before measurement. Fig. 1 shows the relationship of maximum absorbance and the sensitization duration. The adsorption can be divided into three stages. Since the pores in the TiO_2 film are all unoccupied at the initial stage of adsorption, absorbance is increased rapidly, then, the adsorption rate is slowed down with the prolonged sensitization duration. Finally, the adsorption reaches saturation when all active surfaces are occupied. It can be seen from Fig. 1 that the

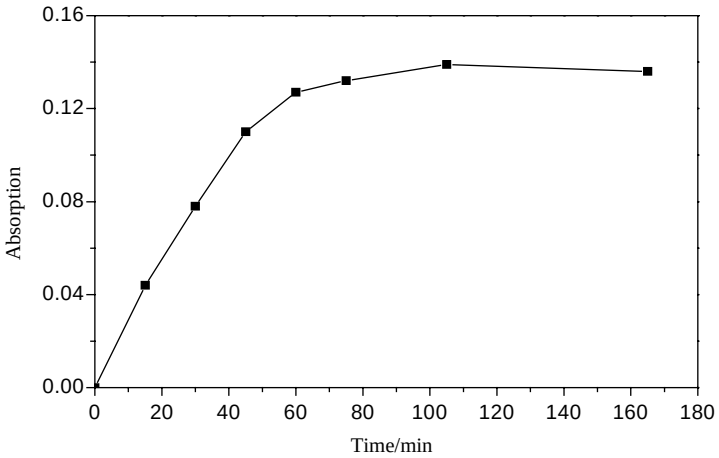

Fig. 1. Relationship of maximum absorption of mN3 and sensitization duration. TiO_2 films used here was about 4μm thick. Absorption of TiO_2 film and glass support was deducted.

optimal duration for sensitization is longer than 100 min. In order to ensure the adsorption saturation, 12 h-sensitization was chosen in this work.

3.2. UV–vis spectra

Absorption properties for the two dyes both in ethanol solutions and on TiO_2 films are listed in Table 1, whereas their absorption spectra are illustrated in Figs. 2 and 3. One can see from Table 1 and Fig. 2 that both the dyes have characteristic $\pi-\pi^*$ electron transition bands around 300 nm and two metal to ligand charge transfer (MLCT) peaks around 400 and 535 nm because of their similar molecular structures. Compared with their corresponding absorption peaks in ethanol solutions, the longer wavelength absorption peaks for the dyes on TiO_2 films (see Fig. 3) are blue-shifted by 53 and 16 nm for N3 and mN3, respectively, suggesting that H-aggregations of the dyes formed on the surface of TiO_2 films. It is notable that the extent of blue-shifting of the peak of mN3 on TiO_2 film is less than that of N3, which is advantageous to the light harvesting. From Table 1, one can see that even though the two dyes have almost the same adsorption amount, the molar extinction coefficient ε for mN3 is smaller than that for N3 by 20–40%, which will be

Table 1
Absorption properties of N3 and mN3

	λ^a max (nm) ($\varepsilon/10^3\,M^{-1}\,cm^{-1}$)	λ^b max (nm)	$\Delta\lambda$ (nm)	N^c (molecules cm^{-2}) film
N3	537 (14.4), 397 (13.4), 313 (49.0)	484	53	1.65×10^{16}
MN3	534 (8.2), 396 (8.2), 298 (27.4)	518	16	1.58×10^{16}

[a] Measured in ethanol solution; molar extinction coefficient values are given in parentheses.
[b] Measured with dye-coated film using conducting glass as reference.
[c] Adsorption amount.

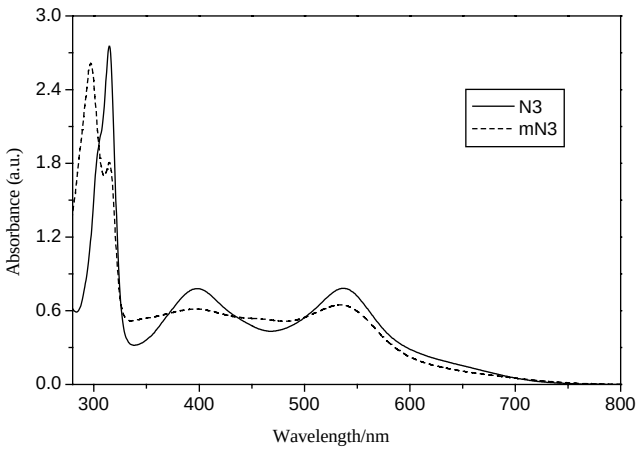

Fig. 2. UV–vis spectra for N3 and mN3 in ethanol solutions.

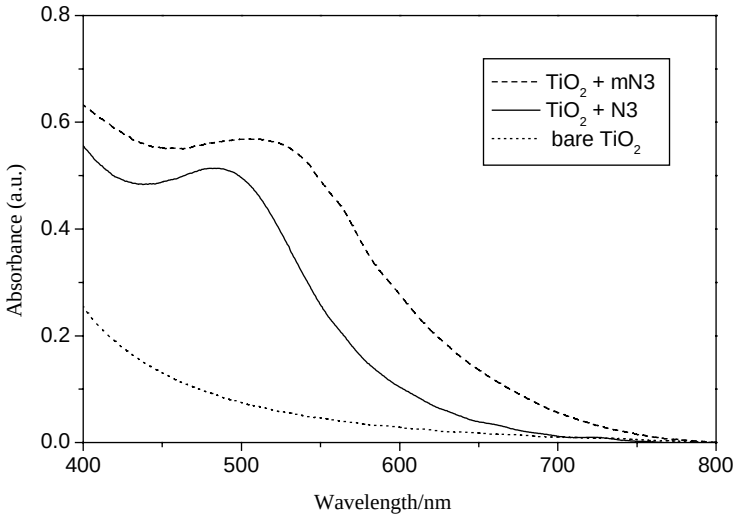

Fig. 3. UV–vis spectra for N3 and mN3 on TiO_2 films, and for bare TiO_2 films, respectively. TiO_2 films used here were about 4 μm thick. Absorption of CTO glass was deducted.

Table 2
Effect of thickness on performance parameters of dye mN3 sensitized solar cells

Thickness (μm)	I_{sc} (mA cm^{-2})	V_{oc} (mV)	ff	η (%)
5.8 (3 layers)	9.5	558	0.54	3.3
8.1 (4 layers)	11.3	573	0.56	4.2
10.0 (5 layers)	11.7	595	0.60	4.6
11.7 (6 layers)	10.2	597	0.65	4.4
14.2 (7 layers)	7.0	583	0.66	3.0

Light intensity was 89.5 mW cm^{-2}.

disadvantageous to the light harvesting, and will consequently reduce the overall energy conversion efficiency of mN3-sensitized solar cell.

3.3. Effect of film thickness on photoelectric conversion

As the film thickness can strongly affect the action spectra and overall energy conversion efficiency, the effect of film thickness on performance parameters of mN3-sensitized solar cells was investigated. Table 2 contains the results for five different films whose thickness varied from 5.8 (3 layers) to 14.2 μm (7 layers). It can be seen from Table 2 that the open-circuit photovoltage (V_{oc}) increased from 558 mV at 5.8 μm to 597 mV at 11.7 μm, then decreased gradually. While short-circuit photocurrent (I_{sc}) attained the highest value around 8–10 μm, then decreased rapidly. Fill factor kept increasing trend while the films become thicker. The fill factor is defined as follows:

$$\mathrm{ff} = V_{opt} I_{opt} / V_{oc} I_{sc} \quad (1)$$

where V_{opt} and I_{opt} are the voltage and current for maximum power output, respectively. η is defined as the following equation:

$$\eta = V_{opt} I_{opt} / P_{in}, \tag{2}$$

where P_{in} is the power of incident white light. As a consequence, the overall energy conversion yield (η) increased from 3.3% at 5.8 μm to the highest value of 4.6% at 10.0 μm and then decreased gradually. The above results show that there is an optimal thickness for the dye-sensitized solar cell. The thinner film adsorbs fewer dye molecules and hence generates lower efficiency. On the contrary, there will be an increasing probability of charge recombination and the cell resistance will become larger when the film thickness is increasing. Since the electron has, on average, to transport across an increasing number of colloidal particles and grain boundaries. On the other hand, in the case of illumination through the support of a substrate, dye molecules adsorbed in the outer part (i.e., the part far from CTO glass) of TiO_2 film will absorb less visible light with increasing film thickness, as the dye adsorbed in the inner part (i.e., the part adjacent to CTO glass) prevents light penetrating deeper. Balancing all of the factors, 10-μm-thick film was chosen to carry out all of the experiments unless otherwise specified.

3.4. Photoelectrochemical behavior

Photocurrent action spectra and photocurrent–voltage characteristics obtained with nanocrystalline TiO_2 films loaded with N3 and mN3 are shown in Figs. 4 and 5, respectively. The monochromatic incident photo-to-electron conversion efficiency (IPCE), defined as the number of electrons generated by light in the outer circuit divided by the number of incident photons, was obtained by means of the following

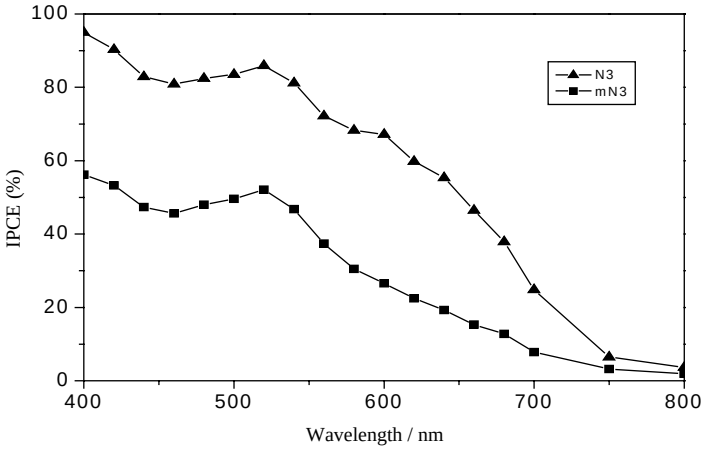

Fig. 4. Photocurrent action spectra for N3 and mN3. IPCE was corrected for the absorption and reflection by CTO glass.

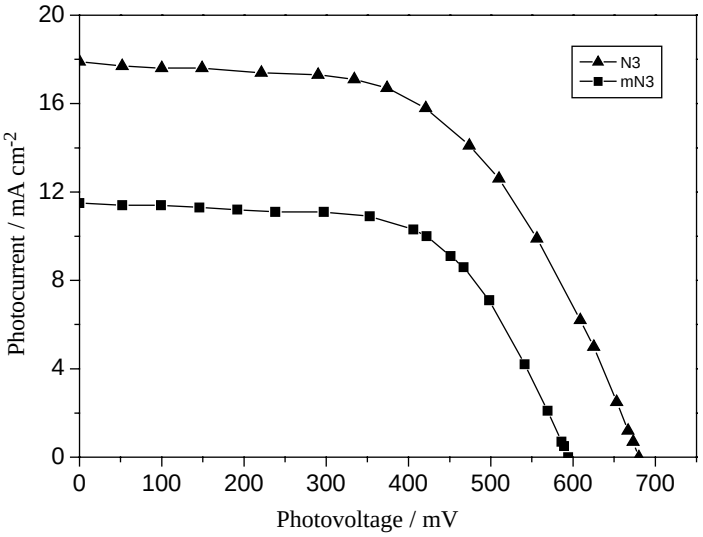

Fig. 5. The $I-V$ curves for N3 and mN3. Solar cells were illuminated under white light of 89.5 mW cm^{-2} from a xenon lamp.

Table 3
Performance characteristics of photovoltaic cells based on nanocrystalline TiO_2 films sensitized by N3 and mN3, respectively

	I_{sc} (mA cm^{-2})	V_{oc} (mV)	ff	η (%)
N3	17.9	698	0.56	7.4
MN3	11.7	595	0.60	4.6

equation:

$$\text{IPCE (\%)} = \frac{1240 I_{sc}\ (\mu\text{A cm}^{-2})}{\lambda\ (\text{nm}) P_{in}\ (\text{W m}^{-2})} \tag{3}$$

where the constant 1240 is derived from units conversion, I_{sc} is the short-circuit photocurrent generated by monochromatic light, and λ is the wavelength of incident monochromatic light, whose light intensity is P_{in}. Fig. 4 presents the action spectra for N3 and mN3. The maximum IPCE was about 56.2%. IPCE over 40% was covered in the range from 400 to 550 nm. The overall conversion efficiency η is 4.6% (see Table 3).

The effect of light intensity on short-circuit photocurrent was examined, as seen in Fig. 6. The short-circuit photocurrents increase linearly with light intensities, indicating that photocurrent generation is not limited by diffusion of the iodide or triiodide ions within the nanocrystalline film in the light intensity range studied.

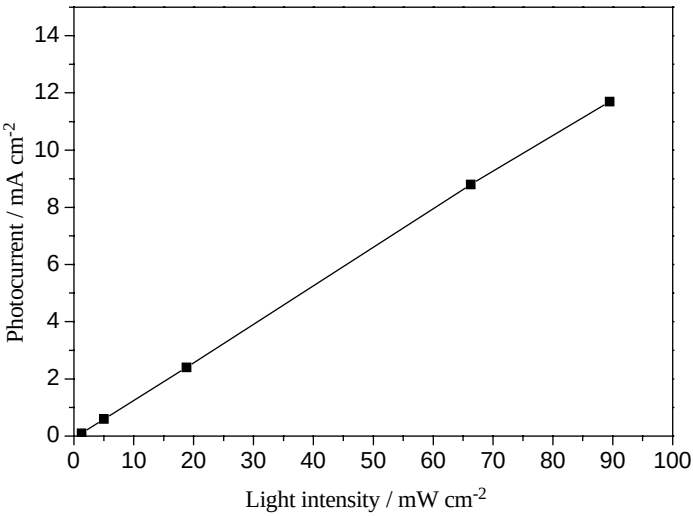

Fig. 6. Relationship between light intensity and the short-circuit photocurrent generated by mN3-sensitized solar cells.

Table 4
Transient properties of N3 and mN3 in ethanol, on TiO_2 films, and as sensitizers in solar cells

	N3 (in ethanol)	mN3 (in ethanol)	N3 (on TiO_2 film)	mN3 (on TiO_2 film)
Life time τ (ns) (298 K)	55	10	11	6.5
Transient IPCE (%) (298 K)	—	—	41.9	32.3

3.5. Synchrotron radiation photoelectron spectroscopy (SRPES)

In order to better understand the electron-injection driving force from the excited state of N3 and mN3 to the conduction band of TiO_2, SRPES was measured, from which the first ionization energy 5.3 and 5.2 eV for N3 and mN3, respectively, were obtained. Because absorption thresholds for both dyes are about 800 nm (1.55 eV), the first excited-state energy levels on the absolute scale are -3.75 and -3.65 eV, respectively. Obviously, the excited-state energy levels of the two dyes both lie above the conduction band edge of TiO_2 (-4.40 eV) [12] when they were excited by visible light, indicating electron injection from excited dye to the conduction band of TiO_2 thermodynamically possible for both dyes.

3.6. Excited-state life times

The transient properties of N3 and mN3 in ethanol solutions, on TiO_2 films, and as the sensitizer in two electrode photovoltaic devices were examined by laser technique and the results are listed in Table 4. In ethanol solution, lifetime of 55 ns for N3 was obtained, which is in accordance with the value 50 ns reported by Grätzel [2].

Under the same conditions, the lifetime of the excited mN3 is 10 ns while the lifetimes for N3 and mN3 on TiO_2 films are 11 and 6.5 ns, respectively. Comparing the former and later, one can see that lifetime of the excited state of the two dyes decreased dramatically when adsorbing on the TiO_2 films, indicating that a quick electron injection from excited-state dye to the conduction band of TiO_2 films happened in both cases. Secondly, it is worthy to note that no matter in ethanol solutions or on the TiO_2 films, the life time of the excited state of N3 is much longer than that of mN3, implying that there exists other pathway for excited mN3 dye to decay. This might be the main reason for the lower overall energy conversion of mN3-sensitized solar cell compared with that of N3.

3.7. Transient photocurrent

The transient photocurrent generated from N3- or mN3-sensitized TiO_2 electrodes after laser excitation is shown in Fig. 7. Integrating the area under the two curves in Fig. 6 yields an electrical charge of $Q = 4.1\,\mu C$ for N3-sensitized solar cell and $Q = 3.2\,\mu C$ for mN3-sensitized solar cell, corresponding to the amount of output electrons n_e 2.6×10^{13} and 2.0×10^{13}, respectively. The laser pulse energy of $23\,\mu J$ at 532 nm corresponds to the amount of input photon n_p 6.2×10^{13} for both cases. According to the definition of IPCE, we have the following equation:

$$\mathrm{IPCE} = n_e/n_p \tag{4}$$

Obviously incident photon to current efficiency of 41.9% and 32.3% at 532 nm are obtained for solar cells sensitized with N3 and mN3, respectively. It is noted that

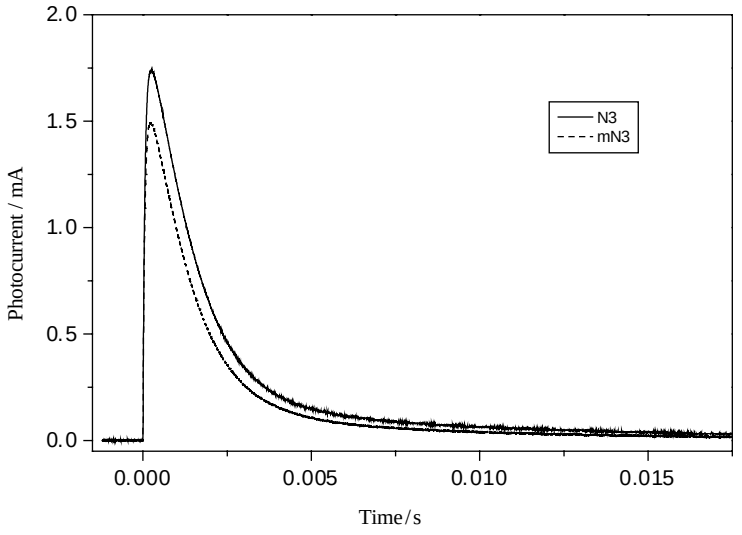

Fig. 7. Time-dependent photocurrent decay curves for solar cells sensitized by N3 and mN3, respectively. Illuminated from the substrate side with 532 nm laser ($23\mu J\,pulse^{-1}$).

under continuous illumination, IPCE of 80% and 48% were measured at 532 nm for N3- and mN3-sensitized solar cells, respectively.

Generally speaking, lower IPCE under laser flash excitation compared to that obtained under continuous illumination maybe caused by the following factors. Firstly, in the case of laser flash the light passes the electrode once while under continuous illumination the light is reflected by the Pt layer deposited on ITO to pass the electrode for a second time or more. Secondly, under pulsed illumination recombination rate is much higher because of very high cation radical and trapped electron concentration created by the intense laser flash. Thirdly, one has to consider that the strong electron injection after high-power laser excitation causes a negative shift of the quasi-Fermi level in the semiconductor. This shift usually amounts to several hundred millivolts. Therefore, injection from the sensitizer will soon cease as the quasi-Fermi level approaches the relatively low excited-state level of this sensitizer. All the factors mentioned above result in a lower IPCE obtained from laser flash excitation than that from continuous illumination [20].

The quantum yield of charge injection is given by [2]

$$\Phi_{\mathrm{inj}} = k_{\mathrm{inj}}/(\tau^{-1} + k_{\mathrm{inj}}) \tag{5}$$

where k_{inj} is the rate constant for electron injection and τ is the excited-state life time in the absence of injection. Using electron injection with a rate constant exceeding about $1 \times 10^{12}\,\mathrm{s}^{-1}$ [21], and transient absorption data in Table 4 results in remarkably high electron-injection efficiency of >0.9 for both N3- and mN3-sensitized solar cells. Since electrons injected either from dye N3 or from dye mN3 transport through the same interconnected nanocrystalline TiO_2 thin film network. So the lower IPCE for mN3 might come from slower electron transfer from the iodide redoxactive electrolyte to the dye cation [22].

4. Conclusions

A new dye, cis-dithiocyanato-(4,4′-dicarboxyl-2,2′-bipyridyl)-(4,4′-di ((N,N′-methylphenylamino)methylene)-2,2′-bipyridyl) Ru(II), was designed and synthesized. Its absorption spectrum, photoelectrical properties, energy level of HOMO, excited-state life time, and transient photocurrent were examined and compared with the star dye N3 under the same experimental conditions. Data imply that the replacement of two carboxylic groups at 4,4′ positions of 2,2-bipyridine by electronic pushing group, methylphenylamino methylene, brings about large changes on photoelectronic conversion. The key factor of all the changes is that the replacement represses the MLCT. These results obtained will be helpful for molecular design of dyes based on ruthenium polypyridine for solar cells.

Acknowledgements

The State Key Program of Fundamental Research (G1998016308), the NNSFC (20023005,59872001 and 29971031), and Doctoral Program of Higher Education (99000132) are gratefully acknowledged for the financial support.

References

[1] B. O'Regan, M. Grätzel, Nature (London) 353 (1991) 737.
[2] M.K. Nazeeruddin, A. Kay, I. Rodicio, R. HumphryBaker, E. Müler, N. Vlachopoulos, M. Grätzel, J. Am. Chem. Soc. 115 (1993) 6382.
[3] C.J. Barbé, F. Arendse, P. Comte, M. Jirouse, F. Lenzmann, V. Shklover, M. Grätzel, J. Am. Ceram. Soc. 80 (1997) 3157.
[4] Zhong-Sheng Wang, Chun-Hui Huang, Yan-Yi Huang, Yuan-Jun Hou, Pu-Hui Xie, Bao-Wen Zhang, Hu-Min Cheng, Chem. Mater. 13 (2001) 678.
[5] R.A. Caruso, M. Antonietti, M. Giersig, H.P. Hentze, J.–G. Jia, Chem. Mater. 13 (2001) 1114.
[6] Md.K. Nazeeruddin, P. Pechy, T. Renouard, S.M. Zakeeruddin, R. Humphry-Baker, P. Comte, P. Liska, L. Cevey, E. Costa, V. Shklover, L. Spiccia, G.B. Deacon, C.A. Bignozzi, M. Grätzel, J. Am. Chem. Soc. 123 (2001) 1613.
[7] A. Hagfeldt, M. Grätzel, Acc. Chem. Res. 33 (2000) 269.
[8] S.M. Zakeerudin, Md.K. Nazeeruddin, R. Humphry-Baker, M. Grätzel, Inorg. Chim. Acta 296 (1999) 250.
[9] T.A. Heimer, S.T. D'Arcangelis, F. Farzad, J.M. Stipkala, G.J. Meyer, Inorg. Chem. 35 (1996) 5319.
[10] R. Argazzi, C.A. Bignozzi, T.A. Heimer, F.N. Castellano, G.J. Meyer, J. Phys. Chem. B 101 (1997) 2591.
[11] P. Pechy, F.P. Rotzinger, Md.K. Nazeeruddin, O. Kohle, S.M. Zakeerudin, R. Humphry-Baker, M. Grätzel, J. Chem. Soc. Chem. Commun. 1 (1995) 65.
[12] A. Hagfeldt, M. Grätzel, Chem. Rev. 95 (1995) 49.
[13] A. Hagfeldt, S.-E. Lindquist, M. Grätzel, Sol. Energy Mater. Sol. Cells 32 (1994) 245.
[14] S.Y. Huang, G. Schlichthorl, A.J. Nozik, M. Grätzel, A.J. Frank, J. Phys. Chem. B 101 (1997) 2576.
[15] S.A. Haque, Y. Tachibana, R.L. Willis, J.E. Moser, M. Grätzel, D.R. Klug, J.R. Durrant, J. Phys. Chem. B 104 (2000) 538.
[16] S. Pelet, J.E. Moser, M. Grätzel, J. Phys. Chem. B 104 (2000) 1791.
[17] S. Nakade, S. Kambe, T. Kitamura, Y. Wada, S. Yanagida, J. Phys. Chem. B 105 (2001) 9150.
[18] Lin-Qing Song, Bao-Wen Zhang, Chinese J. Chemistry, to be published.
[19] Zhong-Sheng Wang, Fu-You Li, Chun-Hui Huang, Lu Wang, Mei Wei, Lin-Pen Jin, Nan-Qiang Li, J. Phys. Chem. B 104 (2000) 9676.
[20] A. Kay, R. Humphry-Baker, M. Grätzel, J. Phys. Chem. 98 (1994) 952.
[21] C.A. Kelly, G.J. Meyer, Coord. Chem. Rev. 211 (2001) 295.
[22] Y. Tachibana, S.A. Haque, I.P. Mercer, J.R. Durrant, D.R. Klug, J. Phys. Chem. B 104 (2000) 1198.